

Brain TSPO-PET predicts later disease progression independent of relapses in multiple sclerosis

Marcus Sucksdorff,^{1,2} Markus Matilainen,¹ Jouni Tuisku,¹  Eero Polvinen,^{1,2} Anna Vuorimaa,^{1,2} Johanna Rokka,¹  Marjo Nylund,¹ Eero Rissanen^{1,2} and Laura Airas^{1,2}

Overactivation of microglia is associated with most neurodegenerative diseases. In this study we examined whether PET-measurable innate immune cell activation predicts multiple sclerosis disease progression. Activation of microglia/macrophages was measured using the 18-kDa translocator protein (TSPO)-binding radioligand ¹¹C-PK11195 and PET imaging in 69 patients with multiple sclerosis and 18 age- and sex-matched healthy controls. Radioligand binding was evaluated as the distribution volume ratio from dynamic PET images. Conventional MRI and disability measurements using the Expanded Disability Status Scale were performed for patients at baseline and 4.1 ± 1.9 (mean ± standard deviation) years later. Fifty-one (74%) of the patients were free of relapses during the follow-up period. Patients had increased activation of innate immune cells in the normal-appearing white matter and in the thalamus compared to the healthy control group ($P = 0.033$ and $P = 0.003$, respectively, Wilcoxon). Forward-type stepwise logistic regression was used to assess the best variables predicting disease progression. Baseline innate immune cell activation in the normal-appearing white matter was a significant predictor of later progression when the entire multiple sclerosis cohort was assessed [odds ratio (OR) = 4.26; $P = 0.048$]. In the patient subgroup free of relapses there was an association between macrophage/microglia activation in the perilesional normal-appearing white matter and disease progression (OR = 4.57; $P = 0.013$). None of the conventional MRI parameters measured at baseline associated with later progression. Our results strongly suggest that innate immune cell activation contributes to the diffuse neural damage leading to multiple sclerosis disease progression independent of relapses.

1 Turku PET Centre, Turku University Hospital and University of Turku, Turku, Finland

2 Division of Clinical Neurosciences, Turku University Hospital, and University of Turku, Turku, Finland

Correspondence to Laura Airas

Turku PET Centre, Turku University Hospital and University of Turku

Po Box 52, 20521 Turku, Finland

E-mail: laura.airas@utu.fi

Keywords: PET imaging; TSPO; microglia; progressive multiple sclerosis; prediction

Abbreviations: ARR = annualized relapse rate; DMT = disease modifying treatment; DVR = distribution volume ratio; EDSS = expanded disability status scale; NAWM = normal appearing white matter

Introduction

Eighty-five per cent of patients with multiple sclerosis present initially with relapsing-remitting disease. Here, the

disease pathogenesis is driven by the peripheral immune system with lymphocytes and monocytes entering the CNS and forming focal inflammatory infiltrates (Compston and Coles, 2008). This aspect of the disease can be reliably monitored

Received December 11, 2019. Revised July 3, 2020. Accepted July 10, 2020. Advance access publication October 2, 2020

© The Author(s) (2020). Published by Oxford University Press on behalf of the Guarantors of Brain.

This is an Open Access article distributed under the terms of the Creative Commons Attribution Non-Commercial License (<http://creativecommons.org/licenses/by-nc/4.0/>), which permits non-commercial re-use, distribution, and reproduction in any medium, provided the original work is properly cited. For commercial re-use, please contact journals.permissions@oup.com

using conventional MRI, and is efficiently controlled using immunomodulatory and immunosuppressive treatments. Recent evidence shows that in addition to the adaptive immune activity, another simultaneous detrimental pathological mechanism is ongoing from the disease onset. This second global process of tissue injury is more diffuse and likely contributes to development of brain atrophy and disability from early on (De Stefano *et al.*, 2010).

The diffuse, widespread tissue injury becomes clinically most prominent within 15–20 years from the disease onset, when the rate of progression seems to increase, while relapses are reduced at the same time (Confavreux *et al.*, 1980; Minderhoud *et al.*, 1988; Weinshenker *et al.*, 1989; Eriksson *et al.*, 2003; Vukusic and Confavreux, 2003; Tremlett *et al.*, 2008; Tutuncu *et al.*, 2013; Cree *et al.*, 2019). Several factors, such as diminishing oestrogen levels among female patients with multiple sclerosis, and the inherent tendency of gradually increasing microglial activation with ageing even in healthy individuals, likely contribute to the more rapid accrual of disability around the age of 45 (Scalfari *et al.*, 2011). Clinical symptoms related to disease progression include progressive loss of walking ability, bladder dysfunction and increasing cognitive impairment. Progression can also occur from the disease onset (primary progressive multiple sclerosis) (Thompson *et al.*, 2018).

The mechanisms behind the development of the insidious, silent progression independent of relapse activity are unclear, but it appears that in progressive multiple sclerosis, the innate immune system within the CNS adopts a pro-inflammatory phenotype. The current understanding is that microglia, macrophages and astrocytes in the normal-appearing white matter (NAWM) and grey matter, and at the rim of chronic active/smoldering lesions secrete pro-inflammatory cytokines and reactive oxygen species, which promote increasing neuro-axonal damage both in the white and grey matter, and this leads to brain and spinal cord atrophy (Gandhi *et al.*, 2010; Ransohoff *et al.*, 2015). The exact mechanisms leading to death of neurons and loss of axons are poorly understood, but oxidative stress and glutamate toxicity have been shown to contribute to mitochondrial dysfunction, which in turn leads to cellular death (Fischer *et al.*, 2012; Campbell *et al.*, 2014).

The ability to identify and effectively manage patients, who are at risk of disability worsening and secondary progressive multiple sclerosis conversion represents a major unmet need. Disease course of multiple sclerosis is highly variable, and patients can present with anything from benign courses that will never convert to secondary progression, to highly active courses with rapid disability progression. There are currently no widely applicable validated biomarkers predicting multiple sclerosis progression, although several papers have recently shed light on this matter (Soelberg Sorensen and Sellebjerg, 2016; Barro *et al.*, 2018; Bhan *et al.*, 2018; Varhaug *et al.*, 2018; Ferraro *et al.*, 2019; Kuhle *et al.*, 2019). Therefore, predictive biomarkers for short-term progression are sorely needed.

Mitochondrial 18-kDa translocator protein (TSPO) is a marker of inflammation commonly attributed to microglial and macrophage activation in neurodegenerative and neuro-inflammatory diseases such as multiple sclerosis (Hogel *et al.*, 2018; Guilarte, 2019). PET imaging using radioligands binding to the TSPO can be used to detect innate immune cell activation *in vivo* in various relevant regions of interest within the brain of patients with multiple sclerosis. However, the significance of the PET-measurable microglial/macrophage activation is not clear in terms of later clinical disease worsening.

The aim of this single-centre study was to assess the usefulness of TSPO-PET imaging for predicting later multiple sclerosis progression. We investigated whether TSPO binding, MRI lesion load or the degree of brain atrophy correlated with progression during a 4-year follow-up period. The findings were confirmed by using stepwise logistic regression where demographic and clinical disease-related variables, conventional MRI variables and treatments were used as potential covariates.

Materials and methods

Study subjects and procedures

The study cohort consisted initially of 73 patients with multiple sclerosis (49 with relapsing-remitting and 24 with secondary progressive multiple sclerosis). Four patients with relapsing-remitting multiple sclerosis were lost to follow-up and were excluded from this study. A group of 18 age- and sex-matched healthy control subjects was included for imaging comparisons.

Expanded Disability Status Scale (EDSS) score was evaluated by experienced clinicians (M.S., E.R., L.A., A.V.) at baseline and after an average of 4.1 (± 1.9), mean (\pm standard deviation, SD), years later, using a standardized examination form, the Neurostatus (neurostatus.net). Confirmed disability worsening was defined as an EDSS increase of 1.0 point (and 0.5 point if baseline EDSS was ≥ 6.0). In all cases where an EDSS increase was noted, the EDSS measurement was confirmed by re-evaluation after 6 months. The annualized relapse rate (ARR) was determined for (i) the follow-up period; and (ii) for the disease history from the diagnosis to the time of PET imaging. Patients were recruited from the outpatient clinic of the Division of Clinical Neurosciences at the University Hospital of Turku, Finland during 2011–2017. All participants provided written informed consent according to the Declaration of Helsinki, with approval by the Ethics Committee of the Hospital District of Southwest Finland. Exclusion criteria included clinical relapse and/or corticosteroid treatment within 30 days of evaluation and of EDSS re-evaluation, and gadolinium contrast enhancement in baseline conventional MRI to avoid confounding effects of acute inflammation on innate immune cell activation and on the evaluation of later progression. Exclusion criteria also included active neurological or autoimmune disease other than multiple sclerosis or another comorbidity considered significant, inability to tolerate PET or conventional MRI, and a current or desired pregnancy.

MRI acquisition and data analysis

For the evaluation of multiple sclerosis pathology and for the acquisition of anatomic reference for the PET images, conventional MRI was performed with a 3 T Ingenuity TF PET/MR scanner (Philips) at baseline as previously described (Bezukladova *et al.*, 2020). The following conventional MRI sequences were used for image acquisition: axial T₂, 3D FLAIR, 3D T₁, and 3D T₁ with gadolinium enhancement. A semi-automated method was used first to create a combined T₂ lesion mask. This was a base for a manually shaped combined T₁ lesion mask, which then was used to create the perilesional region of interest. We have used this method previously (Rissanen *et al.*, 2018), and is described in brief below. A combined T₂ lesion region of interest mask image was identified using the Lesion Segmentation Tool (LST) (www.statistical-modelling.de/lst.html, a toolbox running in SPM8) (Schmidt *et al.*, 2012) as described previously (Rissanen *et al.*, 2018). A combined T₁ lesion region of interest mask image was manually delineated slice by slice, based on the manually corrected T₂ lesion region of interest mask image. The resulting T₁ lesion region of interest mask image was used to fill the corresponding T₁ image with the lesion-filling tool in LST. The filled T₁ was then used for segmenting grey matter, white matter and thalamus with Freesurfer 5.3 software (<http://surfer.nmr.mgh.harvard.edu/>).

T₁ and T₂ lesion loads were measured from manually edited T₁ and T₂ lesion region of interest masks. The perilesional region of interest was created by dilating the corresponding T₁ lesion region of interest mask image by six voxels and then removing the core from the resulting image (= perilesional NAWM). Furthermore, a NAWM region of interest was created by removing the T₁ lesion region of interest and perilesional region of interest from the white matter region of interest.

¹¹C-PK11195 radioligand production and PET image acquisition

The radiochemical synthesis of ¹¹C-PK11195 was performed as described previously (Rissanen *et al.*, 2018). The mean injected dose was 479 (±44) MBq, mean (±SD), for the multiple sclerosis patient group and 490 (±16) MBq for the healthy control group with no significant dose differences between the groups.

PET was performed with a brain-dedicated ECAT High-Resolution Research Tomograph scanner (CTI/Siemens) with an intrinsic spatial resolution of ~2.5 mm. First, a 6-min transmission scan for attenuation correction was obtained using a ¹³⁷Cs point source. Thereafter, 60-min dynamic imaging was started simultaneously with intravenous bolus injection of the radioligand. Head movements were minimized using a thermoplastic mask.

PET post-processing and analysis

PET images were reconstructed using 17 time frames as described previously (Rissanen *et al.*, 2018). The dynamic data were then smoothed using a Gaussian 2.5-mm post-reconstruction filter (Rissanen *et al.*, 2014, 2018). Possible displacements between frames were corrected using mutual information realignment in SPM8. Before modelling, partial volume correction using the Geometric Transfer Matrix method (Rousset *et al.*, 1998) was performed for all regional time activity curves with PETPVE12 toolbox in SPM12 (Gonzalez-Escamilla *et al.*,

2017), where Gaussian function with 2.5 mm full-width at half-maximum was used to approximate the scanner point spread function. Innate immune cell activation was evaluated as specific binding of ¹¹C-PK11195 using distribution volume ratio (DVR) in prespecified regions of interest. For the estimation of the ¹¹C-PK11195 DVR, the time–activity curve corresponding to a reference region devoid of specific TSPO binding was acquired for each PET session using a supervised cluster algorithm with four predefined kinetic tissue classes (SuperPK software) (Turkheimer *et al.*, 2007; Yaqub *et al.*, 2012). The reference tissue–input Logan method with a time interval of 20 to 60 min, was applied to the regional time–activity curves using the supervised cluster algorithm grey reference input.

Statistical analysis

The statistical analyses were performed using R (version 3.6.1). Variables are reported as mean (±SD) unless otherwise stated. Wilcoxon rank-sum test was used to assess the differences in imaging results between the control group and the multiple sclerosis group as well as in initial comparisons of variables between groups with progression or no progression. Spearman correlation was used to assess the relationships between the continuous variables, such as baseline DVR measurements, brain volumes and ARR variables. Forward-type stepwise logistic regression was used to assess which variables were best at predicting EDSS increase. Modelling was done first to the whole multiple sclerosis group and then to a subgroup of patients who did not experience relapses during the follow-up. Several DVR, conventional MRI and clinical variables were considered in the model building. The DVR variables were NAWM, perilesional NAWM, T₁ and T₂ lesions, cortical grey matter and thalamus. The volume variables were T₁ and T₂ lesions, cortical grey matter and thalamus as parenchymal fractions (PF), and whole brain volume. Other variables were EDSS, gender, age, disease duration at baseline, time difference between the EDSS measurements, ARR preceding PET imaging, ARR during the follow-up, class of the disease modifying treatment (DMT) at baseline or at most 2 months before and class of the DMT within the first 3 years after multiple sclerosis onset. All DMTs were categorized into three classes: (i) no DMT; (ii) moderate efficacy DMTs (interferons, glatiramer acetate, dimethyl fumarate, fingolimod and teriflunomide); and (iii) high efficacy DMTs (natalizumab, alemtuzumab, ocrelizumab and rituximab) (Scolding *et al.*, 2015).

The model building began with a model without any predictors, and in each step the most suitable variable according to Akaike Information Criterion (AIC) was added to the model. After the final model with the lowest AIC value was established, the model was checked for its assumptions (e.g. multicollinearity, influential values). The estimates for the parameters were then exponentiated to obtain the odds ratios (OR). Because of the range of some continuous variables, the odds ratios for a 0.1-unit increase were calculated for those variables instead of odds ratios for a 1-unit increase.

The chosen model was further validated using a leave-one-out cross validation, in which the probability of the disease progression for each observation was predicted using all other observations. Sensitivity and specificity were calculated using the contingency tables. For this, if the probability of EDSS increase based on the model was closer to one, the observation was classified as a ‘predicted later disease progression’ and if the

probability of EDSS increase was closer to zero, it was classified as ‘disease progression not predicted’. Receiver operating characteristic curve was also estimated along with area under curve (AUC) value.

All tests were two-tailed and a P -value < 0.05 was considered statistically significant for all analyses.

Data availability

Anonymized data not published within the article will be shared over the next 3 years upon request from a qualified investigator.

Results

Demographic and clinical characteristics of participants

Sixty-nine patients with multiple sclerosis and 18 age- and sex-matched healthy controls were included in the study. Mean age of the patients was 46 (± 10) years, mean (\pm SD), their disease duration averaged 13 (± 7) years and their median EDSS score was 3.0 [interquartile range (IQR) 2.5–4.5] at baseline. ARR during the entire disease history before baseline imaging was 0.58 (± 0.97). Of 69 patients, 18 (26%) patients experienced a relapse during the follow-up. Of the 37 relapses experienced by these patients, three were within 6 months (range 4–6 months) of the final EDSS measurement. Altogether 20 patients (29%) experienced disability progression during the follow-up. There were 51 multiple sclerosis patients free of relapses during the follow-up and 11 of them (22%) experienced disability progression. The treatments and the demographic and clinical characteristics and conventional MRI measurements of the different subgroups are shown in Table 1.

Brain TSPO-radioligand uptake in patients with multiple sclerosis and in healthy controls

Multiple sclerosis patients had significantly higher TSPO-binding (reflecting innate immune cell activation) at baseline in the NAWM and thalamus ($P = 0.033$ and $P = 0.003$, respectively; Wilcoxon; Fig. 1A) compared to the healthy control group. No significant difference was observed in TSPO-binding in the cortical grey matter between the groups (Fig. 1A). The TSPO-binding in the various studied regions of interest i.e. the NAWM, perilesional NAWM and T_2 lesion area correlated significantly with each other (Fig. 1B).

Brain TSPO-radioligand uptake at baseline in patients with or without progression at follow-up

Twenty patients experienced disease progression during the follow-up. Their DVR was 1.22 (± 0.05), mean (\pm SD), in the

NAWM and 1.26 (± 0.08) in the perilesional NAWM. This was statistically significantly higher than the respective DVR values among the 49 multiple sclerosis patients not progressing during the follow-up, whose DVR values were 1.19 (± 0.05) in the NAWM and 1.21 (± 0.09) in the perilesional NAWM ($P = 0.01$ and $P = 0.022$, respectively; Wilcoxon; Fig. 2A and B). In other regions of interest no differences in innate immune cell activation were observed between these subgroups (Fig. 2C–F).

Among the 51 patients free of relapses during the follow-up, those 11 experiencing progression had statistically significantly higher mean DVR values in the NAWM and in the perilesional NAWM compared to the respective DVR values in the 40 multiple sclerosis patients not experiencing progression during the follow-up [1.24 (± 0.04) versus 1.19 (± 0.05) in the NAWM and 1.31 (± 0.07) versus 1.21 (± 0.08) in the perilesional NAWM, $P = 0.006$ and $P < 0.001$ respectively; Wilcoxon; Fig. 3A and B]. In other regions of interest, no differences in baseline innate immune cell activation were observed between these subgroups (Fig. 3C–F).

Brain volumetric variables at baseline in patients with or without progression at follow-up

T_1 and T_2 lesion load at baseline conventional MRI imaging was higher in patients who experienced disease progression, compared to those who did not progress ($P = 0.007$ and $P = 0.018$, respectively; Wilcoxon; Fig. 4A and B). Brain volumetric measurements at baseline imaging did not correlate with progression status (Fig. 4C–F).

In the patient group free of relapses during the follow-up, there were no statistically significant differences in conventional MRI lesion loads or brain volumetric measurements between patients experiencing or not experiencing disease progression during the follow-up (Fig. 5A–F).

Prediction of multiple sclerosis progression using TSPO-radioligand uptake and other imaging and clinical variables

In forward type stepwise logistic regression for the entire multiple sclerosis cohort ($n = 69$), EDSS at baseline, TSPO binding in the NAWM, class of the DMT at baseline or at most 2 months before baseline, and ARR during the follow-up remained in the model as predictors. Higher TSPO binding in the NAWM predicted later disease progression (OR = 4.26; $P = 0.048$). High efficacy DMT reduced the odds of later disease progression significantly, compared to no DMT (OR = 0.04; $P = 0.038$). Higher ARR during the follow-up also increased the odds of disease progression (OR = 1.41; $P = 0.012$). In the patient group free of relapses during the follow-up ($n = 51$), higher perilesional NAWM TSPO-binding predicted later disease progression (OR = 4.57;

Table 1 Demographic information, conventional MRI data and clinical variables of the study patients

Variable	All patients	Patients with no relapses during follow-up	Patients with relapses during follow-up	Healthy controls
<i>n</i>	69	51	18	18
Females, <i>n</i> (%)	50 (72)	35 (69)	15 (83)	13 (72)
Age, years	46 (10)	46 (9)	47 (13)	43 (11)
Disease duration, years	13 (7)	12 (7)	15 (9)	N/A
EDSS at baseline, median (IQR)	3.0 (2.5–4.5)	3.0 (2.5–4.25)	3.25 (2.5–5.13)	N/A
T ₂ lesion load (PF), median (IQR)	0.005 (0.003–0.014)	0.005 (0.003–0.013)	0.008 (0.002–0.016)	N/A
T ₁ lesion load (PF), median (IQR)	0.003 (0.001–0.008)	0.003 (0.001–0.008)	0.004 (0.001–0.007)	N/A
NAWM volume (PF)	0.33 (0.04)	0.33 (0.04)	0.32 (0.04)	0.35 (0.03)*
Grey matter volume (PF)	0.31 (0.03)	0.31 (0.02)	0.31 (0.03)	0.33 (0.02)*
Thalamus volume (PF)	0.010 (0.001)	0.010 (0.001)	0.010 (0.001)	0.012 (0.001)*
Whole brain (cm ³)	1134 (109)	1136 (103)	1128 (127)	1205 (110)*
Follow-up duration (years)	4.1 (1.9)	3.9 (1.9)	4.6 (1.8)	N/A
ARR before baseline	0.58 (0.97)	0.49 (0.69)	0.83 (1.53)	N/A
ARR during follow-up	0.13 (0.26)	0	0.49 (0.29)	N/A
DMT at baseline or at most 2 months before, <i>n</i> (%)				
No DMT	26 (38)	18 (35)	8 (44)	N/A
Moderate efficacy DMT	33 (48)	26 (51)	7 (39)	N/A
High efficacy DMT	10 (14)	7 (14)	3 (17)	N/A

*Statistically significantly different values compared to all multiple sclerosis patients and to patients with no relapses, at a level of $P < 0.05$ (Wilcoxon rank-sum test). Variables presented mean (\pm SD) unless stated otherwise.

N/A = not applicable; PF = parenchymal fraction (= volume/intracranial volume).

Table 2 Association between innate immune cell activation and EDSS progression

Predictors in the final model	Stepwise logistic regression		
	Estimate	OR	P-value
All patients (<i>n</i> = 69)			
EDSS at baseline	0.33	1.39	0.102
ARR during follow-up	3.41	1.41 ^a	0.012*
Moderate efficacy DMT ^b	−0.92	0.4	0.228
High efficacy DMT ^c	−3.17	0.04	0.038*
DVR in NAWM	14.5	4.26 ^a	0.048*
Patients not experiencing relapses during the follow-up (<i>n</i> = 51)			
DVR in perilesional NAWM	15.2	4.57 ^a	0.013*
Moderate efficacy DMT ^b	−1.92	0.15	0.044*
High efficacy DMT ^c	−0.65	0.52	0.616

EDSS progression was modelled using forward-type stepwise logistic regression. Here, testing was begun with no variables in the model and the addition of each variable was tested using the Akaike information criterion. Most significant improvement of the fit determined the inclusion of the variable. The process was repeated until no variable improved the model. The table shows the variables that remained in the model at the end. Among the entire multiple sclerosis cohort the first variable chosen by the Akaike information criterion to add to the model was EDSS at baseline and each of the other variables listed in the table further improved the model fit to predict progression. In the cohort with no relapses, the first variable to add to the model was DVR in the perilesional NAWM.

All variables considered in model building are listed in detail in the 'Materials and methods' section. Estimates are logarithmic odds ratios (OR).

^aFor DVR variables and ARR, the odds ratio is calculated as 0.1 unit increase due to the scale of the variables as explained in the 'Materials and methods' section.

^bClass of the DMT at baseline or at most 2 months before: moderate efficacy DMT versus no DMT.

^cClass of the DMT at baseline or at most 2 months before: high efficacy DMT versus no DMT.

*Statistical significance at a level of $P < 0.05$.

$P = 0.013$). Also, moderate efficacy DMT reduced the odds of later disease progression significantly, compared to no DMT (OR = 0.15; $P = 0.044$).

In the entire multiple sclerosis cohort, the final logistic regression model predicted disease progression with 55% sensitivity and 90% specificity with an AUC value of 0.78 (Fig. 6A). In the patient group free of relapses during the follow-up, the final logistic regression model predicted disease progression with 55% sensitivity and 95% specificity with an AUC value of 0.75 (Fig. 6B).

Discussion

The results from this *in vivo* TSPO-PET study demonstrate that increased TSPO-radioligand uptake in the perilesional NAWM predicts later disability progression independent of relapse activity during a 4-year follow-up. This strongly suggests that the TSPO-high phenotype of innate immune cells is a harmful phenomenon contributing to the widespread, diffuse neuroaxonal damage, and to the development of the insidious, silent progression independent of relapse activity. Importantly, the innate immune cell activation seems to have an impact on multiple sclerosis disease evolution also at the earliest stages of the disease as it has been demonstrated that higher microglial/macrophage activation increased the subsequent risk of clinically definite multiple sclerosis in patients with clinically isolated syndrome during a 2-year follow-up (Giannetti et al., 2015).

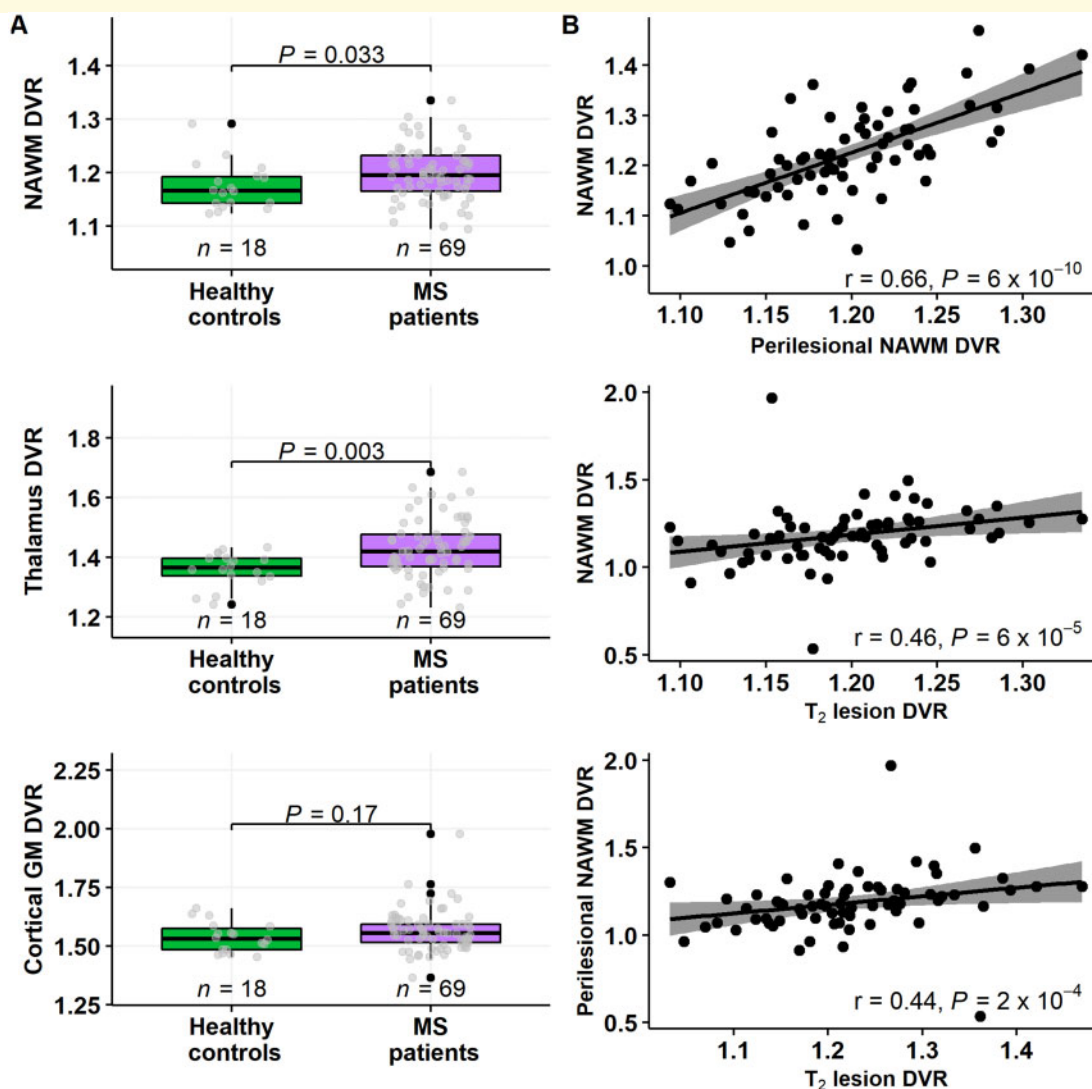


Figure 1 ^{11}C -PK11195 DVR values in various brain regions of interest in multiple sclerosis patients and healthy controls. **(A)** Box plots of the ^{11}C -PK11195 DVR values of patients with multiple sclerosis and healthy controls in the NAWM (top left), in the thalamus and in the cortical grey matter. Evaluation of innate immune cell activation in different brain regions of interest was performed using PET imaging and the ^{11}C -PK11195 radioligand in patients with multiple sclerosis ($n = 69$) and in a healthy control group ($n = 18$). Innate immune cell activation was increased in the NAWM and in the thalamus in patients compared to healthy controls. No statistically significant difference was detected in the cortical grey matter between these groups. Wilcoxon rank-sum test was used for statistical analyses. In box plots the thick horizontal lines represent the medians, the boxes represent the IQR and the end of the whiskers or the points of the outliers represent the minimum and maximum values. **(B)** Correlation between ^{11}C -PK11195 DVR measurements in the different brain regions of interest. DVR values in the NAWM, in the perilesional NAWM and in T_2 lesions correlated highly with each other. Spearman correlation was used for statistical analyses. GM = grey matter; MS = multiple sclerosis.

Recent *ex vivo* immunohistochemical staining and elegant transcriptional profiling of microglia obtained from various regions of human autopsy multiple sclerosis brain have demonstrated an abundance of different microglial phenotypes related to multiple sclerosis pathology (Nutma *et al.*, 2019; van der Poel *et al.*, 2019). TSPO is known to be upregulated in activated glia and macrophages but until now, there has been uncertainty as to the functional nature of the cells detectable by TSPO-PET imaging in multiple sclerosis brain. Given the plethora of the different glial cell phenotypes under diverse CNS pathological conditions, a PET

radioligand will always fall short in comprehensively capturing the features of glial pathology associated with neuroaxonal damage. Importantly, the present study confirms that increased TSPO-binding is an undesired phenomenon, which predicts more rapid multiple sclerosis disease progression.

The first-generation TSPO ligand ^{11}C -PK11195 is the most used radioligand to measure neuroinflammation *in vivo* (Hogel *et al.*, 2018; Guilarte, 2019). Attempts for improved signal-to-noise radioligand properties led to development of second-generation TSPO ligands, which have their drawbacks, such as genetic polymorphism leading to

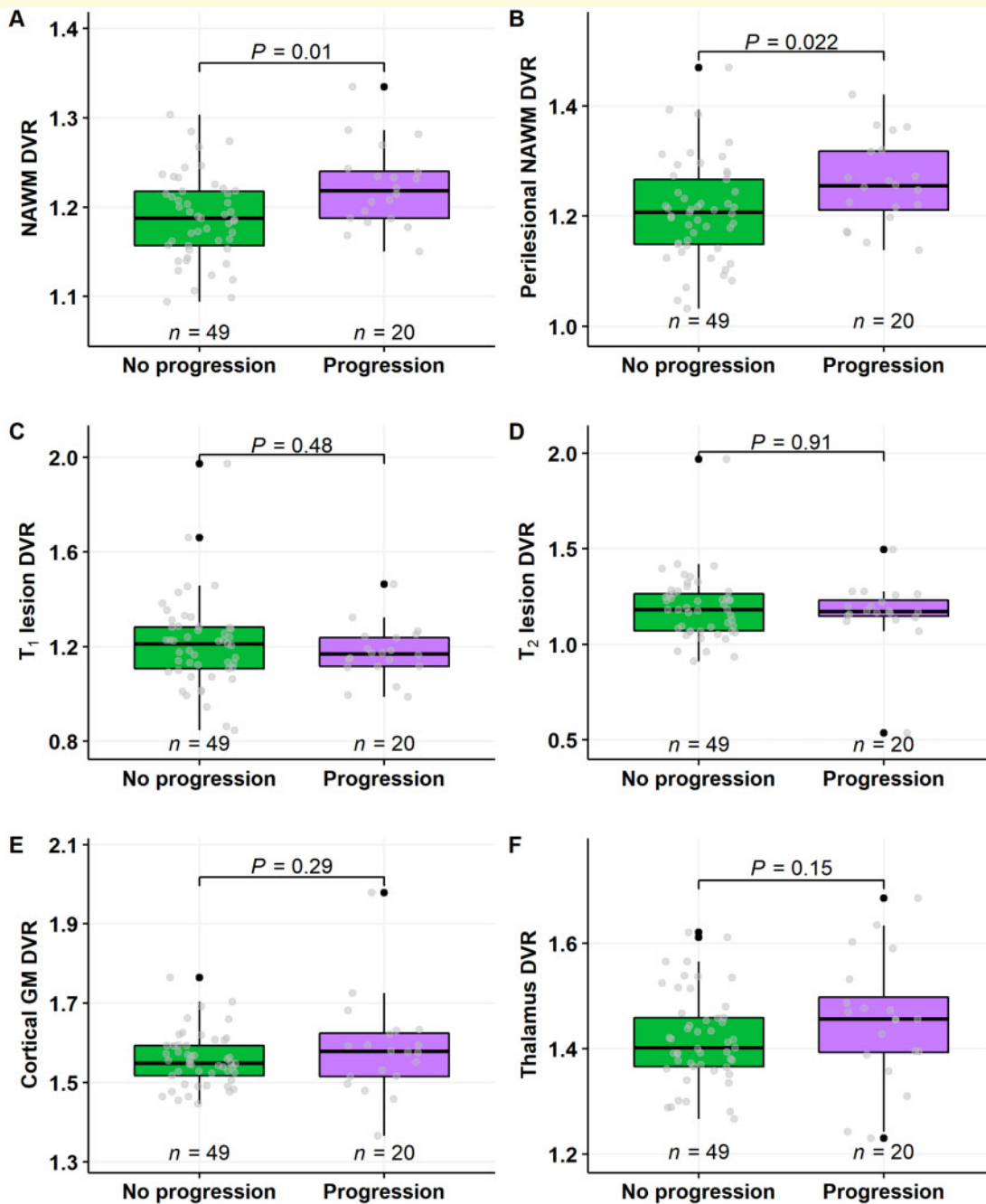


Figure 2 ^{11}C -PK11195 DVR values in multiple sclerosis patients with or without progression during follow-up. Innate immune cell activation was higher both in the NAWM (A) and in the perilesional NAWM (B) in patients who experienced disease progression, compared to those who did not progress, during an average follow-up of 4 years. In other regions of interest, no differences between disease progression and baseline innate immune cell activation was observed (B–F). Wilcoxon rank-sum test was used for statistical analysis. GM = grey matter.

variability in binding affinity between individuals (Owen *et al.*, 2012). Fortunately, the present work, and several earlier studies confirm that ^{11}C -PK11195, despite its shortcomings, can be reliably used to address the ongoing diffuse CNS pathological processes related to multiple sclerosis progression. This can be achieved with careful image acquisition with a high resolution PET camera, and with well validated post-processing and image analysis (Turkheimer *et al.*, 2007;

Politis *et al.*, 2012; Giannetti *et al.*, 2014; Rissanen *et al.*, 2014, 2018; Sucksdorff *et al.*, 2019). In accordance to earlier neuropathological studies (Kutzelnigg *et al.*, 2005), our PET imaging results confirm increased innate immune cell activation both diffusively in the NAWM and in the perilesional area, and activation in both of these regions of interest is associated with later disease progression. While perilesional NAWM TSPO binding was the strongest

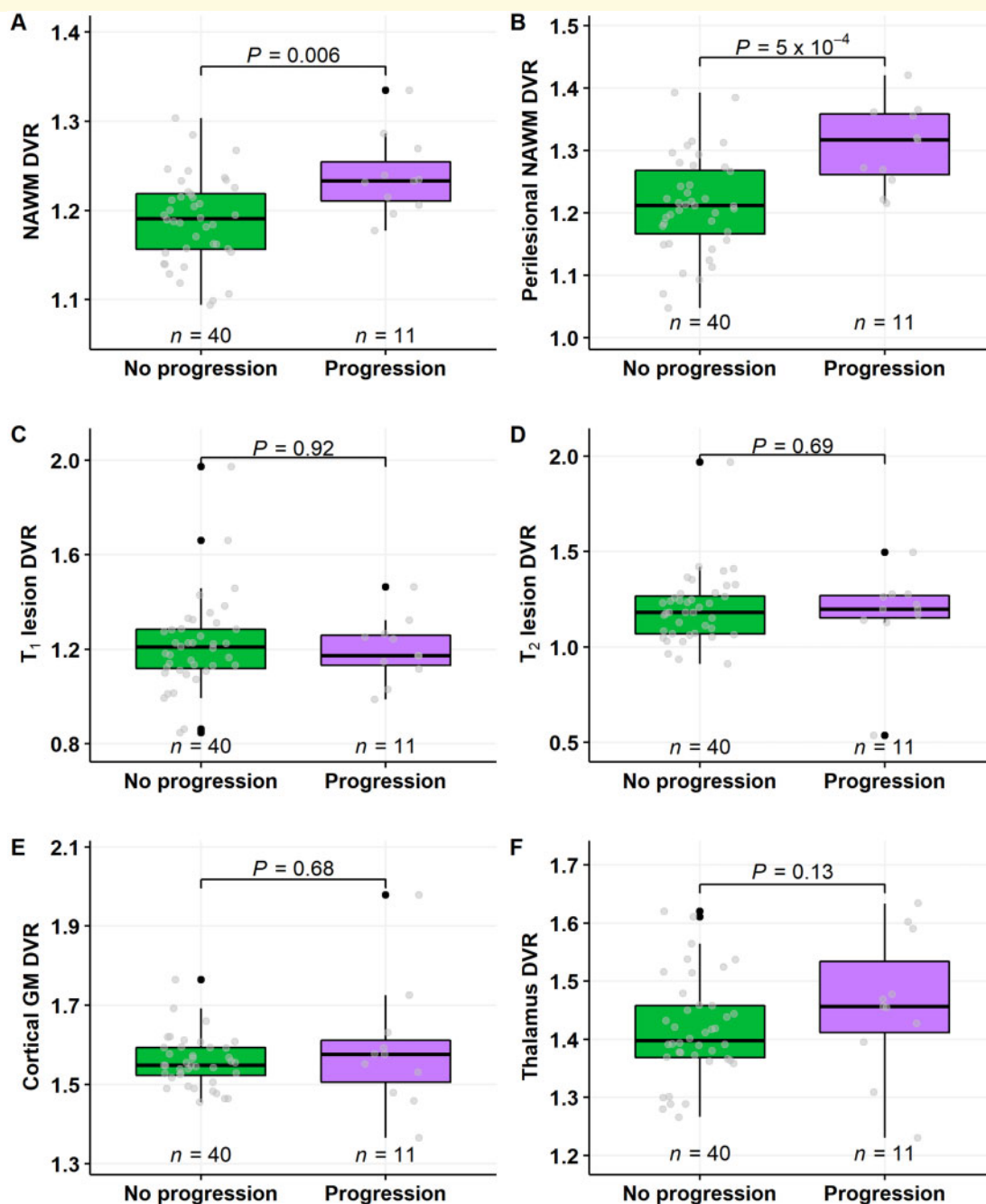


Figure 3 ¹¹C-PK11195 DVR values in multiple sclerosis patients with no relapses and with or without progression during follow-up. Innate immune cell activation was higher both in the NAWM (A) and in the perilesional NAWM (B) in patients who experienced disease progression, compared to those who did not progress. In other regions of interest, no differences between disease progression and baseline innate immune cell activation was observed (B–F). Wilcoxon rank-sum test was used. GM = grey matter.

predictor in the statistical model in the silent progression independent of relapse activity group, and was thus left in the model, it is worth noting that had perilesional NAWM been replaced with NAWM, the TSPO-binding in the NAWM would also have been a significant predictor in the model ($P = 0.023$, data not shown).

Despite the promising results of the present study it must be kept in mind that because of technical challenges and

radiation exposure, TSPO-PET is not a widely usable biomarker in clinical practice, and there is therefore a clear need for biomarkers that relate to innate immune cell activation, but are more easily measurable. Previous attempts to predict multiple sclerosis progression include studies using conventional MRI and blood soluble biomarkers (Goodin, 2006; Fisniku *et al.*, 2008; Kearney *et al.*, 2014; Soelberg Sorensen and Sellebjerg, 2016; Healy *et al.*, 2017; Barro

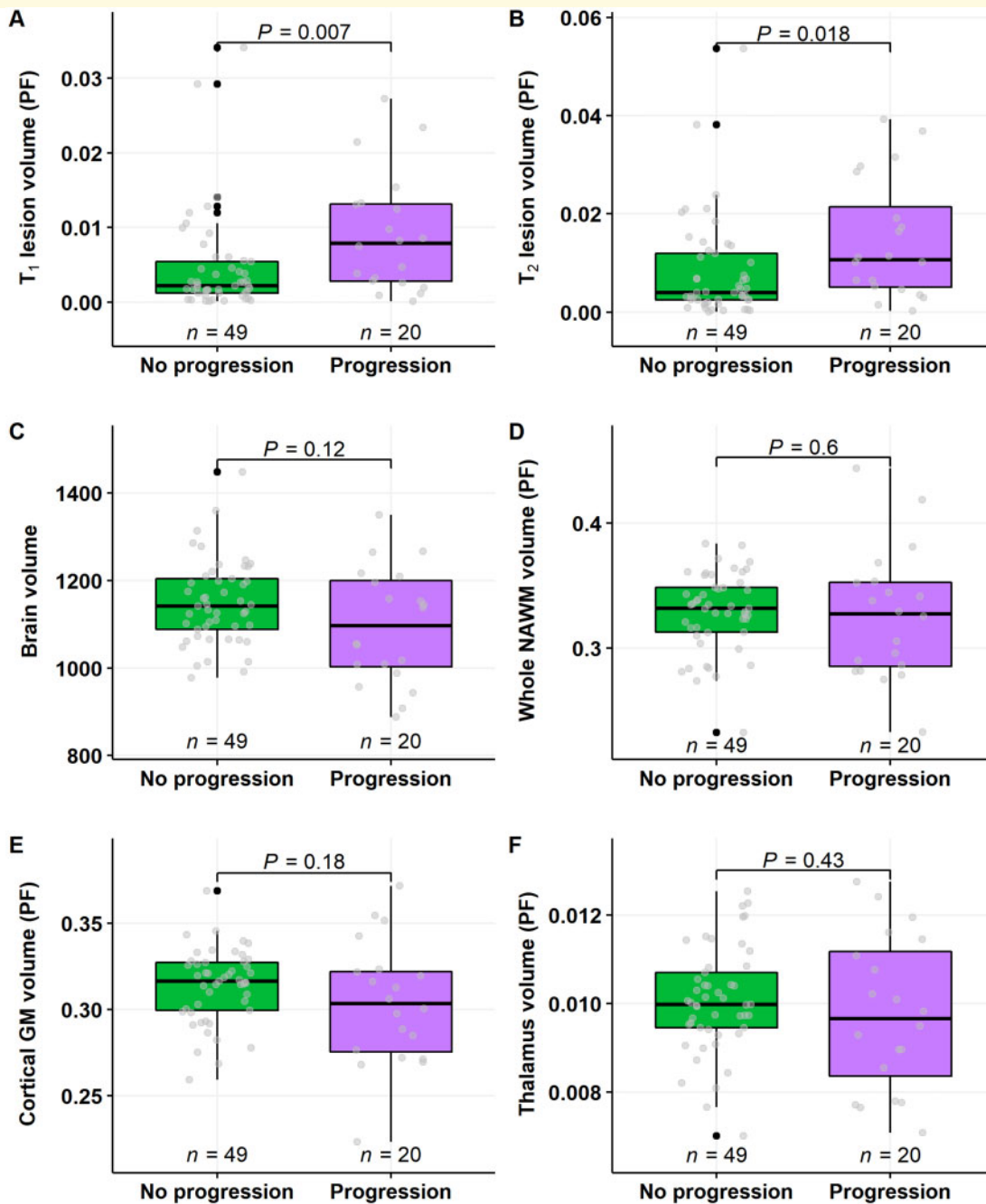


Figure 4 Baseline conventional MRI lesion load and brain volume measurements in multiple sclerosis patients with or without progression during follow-up. T₁ and T₂ lesion load at baseline imaging was higher in patients who experienced disease progression, compared to those who did not progress (A and B). There were no differences in brain volume variables between the groups (C–F). Wilcoxon rank-sum test was used. GM = grey matter; PF = parenchymal fractions.

et al., 2018; Bhan et al., 2018; Varhaug et al., 2018; Ferraro et al., 2019). An association between conventional MRI findings and subsequent disease progression has been demonstrated. Here, brain and upper cervical spinal cord atrophy rate and T₂ lesion volume were the most notable predictors of later progression (Bermel and Bakshi, 2006; Goodin, 2006; Bar-Zohar et al., 2008; Fisniku et al., 2008; Popescu et al., 2013; De Stefano et al., 2014; Jacobsen et al.,

2014; Kearney et al., 2014; Wattjes et al., 2015; Zivadinov et al., 2016; Healy et al., 2017; Casserly et al., 2018; Tsagkas et al., 2018; Andelova et al., 2019). Moreover, a recent study showed an association between ‘atrophied brain T2 lesion volume’ and later disability progression (Genovese et al., 2019), making this quantitative measurement a promising tool for predicting future disease progression (Zivadinov et al., 2018). Neurofilament concentration in

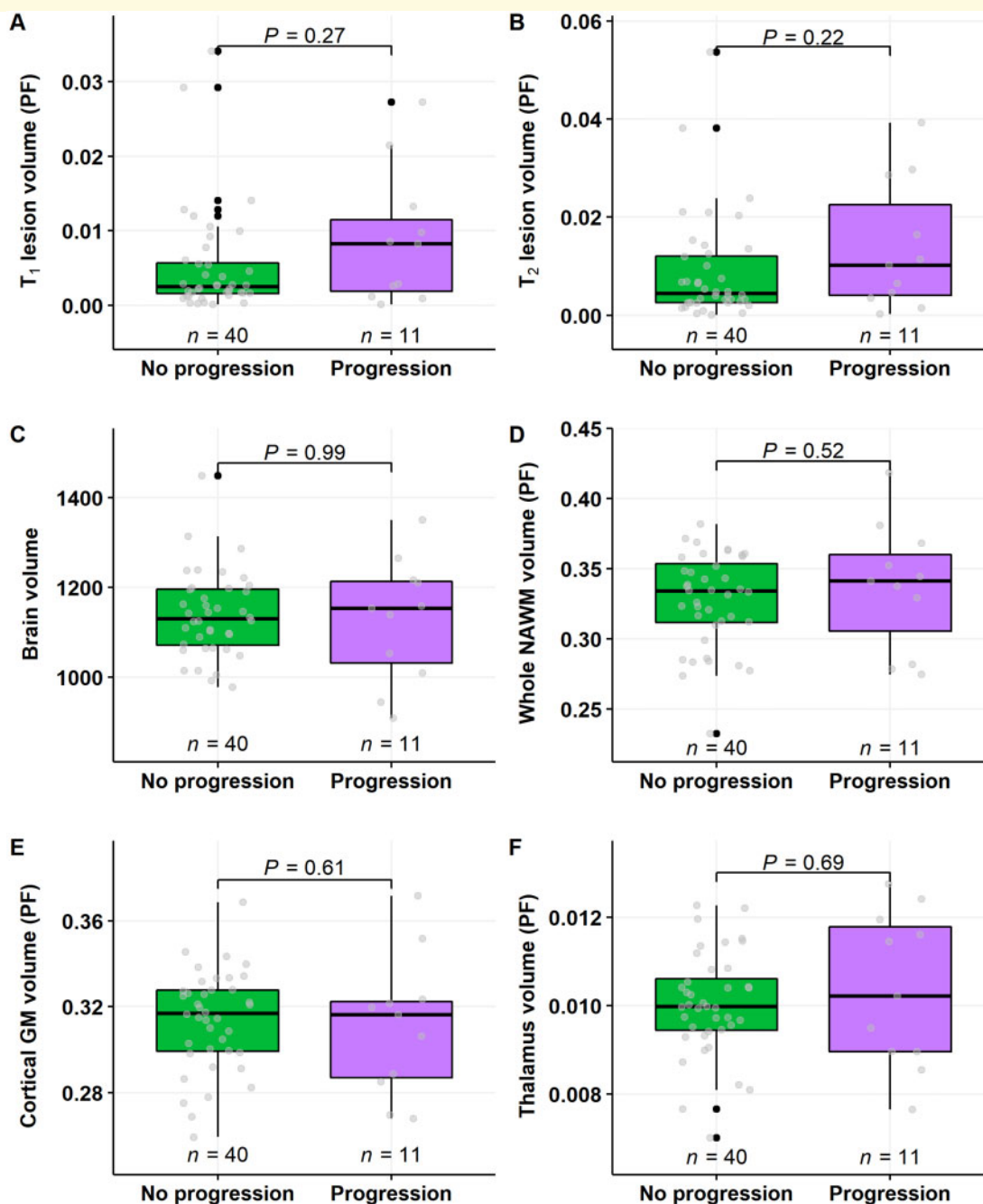


Figure 5 Baseline conventional MRI lesion load and brain volume measurements in multiple sclerosis patients with no relapses and with or without progression during follow-up. There were no statistically significant differences on the conventional MRI volumetric measurements. Wilcoxon rank-sum test was used. GM = grey matter; PF = parenchymal fractions.

blood has similarly been demonstrated as a biomarker for predicting multiple sclerosis progression (Barro *et al.*, 2018). A recent MRI study sought to detect chronic lesion rims with paramagnetic properties, interpreted as presence of iron-containing activated pro-inflammatory microglial cells at the chronic lesion rim (Absinta *et al.*, 2019). In this study, a higher number of rim-active (rim+) chronic lesions associated with earlier and more severe past disability accrual. No prospective analysis of later disability progression following

the detection of rim+ lesions was however performed (Absinta *et al.*, 2019). In the present study, no association was identified between greater T₁ or T₂ lesion load or brain atrophy at baseline, and disability progression during the 4-year follow-up. This may be due to the smaller patient cohort and/or shorter follow-up of the patients compared to the other thus far reported studies (Fisniku *et al.*, 2008; Popescu *et al.*, 2013; Jacobsen *et al.*, 2014; Kearney *et al.*, 2014).

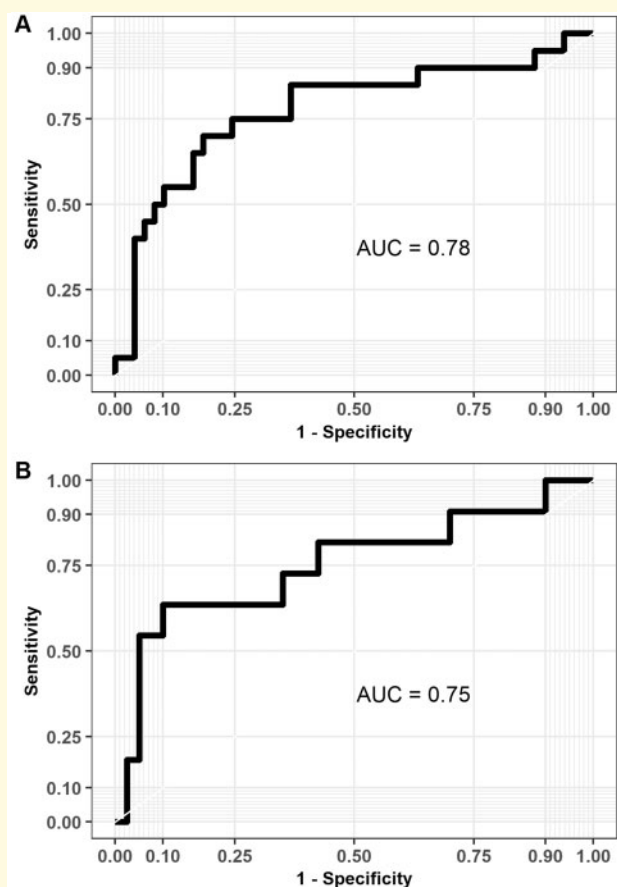


Figure 6 Receiver operating characteristic curves with AUC values based on the predictions from the logistic regression models using leave-one-out cross validation. **(A)** The logistic regression model for the whole multiple sclerosis cohort ($n = 69$) predicted correctly progression in 11/20 patients (sensitivity = 55%) and no progression in 44/49 patients (specificity = 90%). **(B)** The logistic regression model for the cohort without any relapses ($n = 51$) predicted correctly progression in 6/11 patients (sensitivity = 55%) and no progression in 38/40 patients (specificity = 95%).

There are some limitations to our study. The variety of treatments clearly pose a significant confounding factor for evaluation of disease worsening in a real-world setting. In our study, we attempted to carefully control for the confounding effects of the treatments in the regression model. Due to the semi-automated method for identification of lesions and peri-lesional NAWM areas, we could not investigate the impact of individual lesions on disease progression, but instead used regions of interest encompassing all lesions or the entire perilesional area. In future studies it will be important to address also the impact of individual chronic active lesions on disease progression. Another limitation is that the study focuses on brain white matter changes, and has limited information on spinal cord abnormalities or focal grey matter lesions, which are also known to have a significant effect on disability measurement outcomes (Lukas et al., 2013; Harrison et al., 2015).

To conclude, innate immune cell activation is a critical pathological element contributing to disease progression. Our study is, to our knowledge, the first to demonstrate that higher TSPO binding predicts greater clinical disability. Because of high inter-individual variability in multiple sclerosis clinical course and severity, it is a highly attractive prospect to be able to predict which patients have the greatest likelihood of experiencing progressive disability in the near future. It would enable more individualized care in the clinical setting if treatments aiming to slow down progression could be given to a patient population with greatest likelihood of progression. In addition, in clinical trials of progressive disease it would allow more appropriate selection of patients, and would thus improve the success rate of the trials. TSPO-PET imaging has already been applied in treatment trials of neurological disease as an outcome measure (e.g. NCT02481674), but to our knowledge it has not yet been used to enrich the targeted patient population.

Acknowledgements

We want to thank all multiple sclerosis patients participating in this study, and the expert personnel of the Turku PET Centre.

Funding

This work was funded by the Academy of Finland, the Sigrid Juselius foundation, the Finnish MS Foundation and the Finnish Medical Foundation.

Competing interests

M.S. has served on advisory boards for Sanofi-Aventis and Roche, and has received speaker honoraria from Merck Serono and travel honoraria Orion, Roche, Biogen and Sanofi-Aventis and received research support from The Finnish Medical Foundation, The Finnish MS Foundation and from The Finnish Medical Society (Finska Läkaresällskapet); Eero Rissanen has received speaker honoraria from Teva, Biogen, Roche and Merck, and advisory board and consultational fees from Biogen and Merck; L.A. has received honoraria from Biogen, Roche, Genzyme, Merck Serono and Teva, and institutional research grant support from Finnish Academy, Sigrid Juselius Foundation, Nancy Davis Foundation, Biogen, Genzyme, Merck Serono and Novartis.

References

- Absinta M, Sati P, Masuzzo F, Nair G, Sethi V, Kolb H et al. Association of chronic active multiple sclerosis lesions with disability in vivo. *JAMA Neurol* 2019; 76: 1474–83.
- Andelova M, Uher T, Krasensky J, Sobisek L, Kusova E, Srpova B, et al. Additive effect of spinal cord volume, diffuse and focal cord

- pathology on disability in multiple sclerosis. *Front Neurol* 2019; 10: 820.
- Bar-Zohar D, Agosta F, Goldstaub D, Filippi M. Magnetic resonance imaging metrics and their correlation with clinical outcomes in multiple sclerosis: a review of the literature and future perspectives. *Mult Scler* 2008; 14: 719–27.
- Barro C, Benkert P, Disanto G, Tsagkas C, Amann M, Naegelin Y, et al. Serum neurofilament as a predictor of disease worsening and brain and spinal cord atrophy in multiple sclerosis. *Brain* 2018; 141: 2382–91.
- Bermel RA, Bakshi R. The measurement and clinical relevance of brain atrophy in multiple sclerosis. *Lancet Neurol* 2006; 5: 158–70.
- Bezukladova S, Tuisku J, Matilainen M, Vuorimaa A, Nylund M, Smith S, et al. Insights into disseminated MS brain pathology with multimodal diffusion tensor and PET imaging. *Neurol Neuroimmunol Neuroinflamm* 2020; 7: e691.
- Bhan A, Jacobsen C, Myhr KM, Dalen I, Lode K, Farbu E. Neurofilaments and 10-year follow-up in multiple sclerosis. *Mult Scler* 2018; 24: 1301–7.
- Campbell GR, Worrall JT, Mahad DJ. The central role of mitochondria in axonal degeneration in multiple sclerosis. *Mult Scler* 2014; 20: 1806–13.
- Cassery C, Seyman EE, Alcaide-Leon P, Guenette M, Lyons C, Sankar S, et al. Spinal cord atrophy in multiple sclerosis: a systematic review and meta-analysis. *J Neuroimaging* 2018; 28: 556–86.
- Compston A, Coles A. Multiple sclerosis. *Lancet* 2008; 372: 1502–17.
- Confavreux C, Aimard G, Devic M. Course and prognosis of multiple sclerosis assessed by the computerized data processing of 349 patients. *Brain* 1980; 103: 281–300.
- Cree BAC, Hollenbach JA, Bove R, Kirkish G, Sacco S, Caverzasi E, et al. Silent progression in disease activity-free relapsing multiple sclerosis. *Ann Neurol* 2019; 85: 653–66.
- De Stefano N, Airas L, Grigoriadis N, Mattle HP, O’Riordan J, Oreja-Guevara C, et al. Clinical relevance of brain volume measures in multiple sclerosis. *CNS Drugs* 2014; 28: 147–56.
- De Stefano N, Giorgio A, Battaglini M, Rovaris M, Sormani MP, Barkhof F, et al. Assessing brain atrophy rates in a large population of untreated multiple sclerosis subtypes. *Neurology* 2010; 74: 1868–76.
- Eriksson M, Andersen O, Runmarker B. Long-term follow up of patients with clinically isolated syndromes, relapsing-remitting and secondary progressive multiple sclerosis. *Mult Scler* 2003; 9: 260–74.
- Ferraro D, Guicciardi C, De Biasi S, Pinti M, Bedin R, Camera V, et al. Plasma neurofilaments correlate with disability in progressive multiple sclerosis patients. *Acta Neurol Scand* 2019; 141: 16–21.
- Fischer MT, Sharma R, Lim JL, Haider L, Frischer JM, Drexhage J, et al. NADPH oxidase expression in active multiple sclerosis lesions in relation to oxidative tissue damage and mitochondrial injury. *Brain* 2012; 135 (Pt 3): 886–99.
- Fisniku LK, Brex PA, Altmann DR, Miszkiel KA, Benton CE, Lanyon R, et al. Disability and T2 MRI lesions: a 20-year follow-up of patients with relapse onset of multiple sclerosis. *Brain* 2008; 131 (Pt 3): 808–17.
- Gandhi R, Laroni A, Weiner HL. Role of the innate immune system in the pathogenesis of multiple sclerosis. *J Neuroimmunol* 2010; 221: 7–14.
- Genovese AV, Hagemeyer J, Bergsland N, Jakimovski D, Dwyer MG, Ramasamy DP, et al. Atrophied brain T2 lesion volume at MRI is associated with disability progression and conversion to secondary progressive multiple sclerosis. *Radiology* 2019; 190306.
- Giannetti P, Politis M, Su P, Turkheimer F, Malik O, Keihaninejad S, et al. Microglia activation in multiple sclerosis black holes predicts outcome in progressive patients: an in vivo [(11)C](R)-PK11195-PET pilot study. *Neurobiol Dis* 2014; 65: 203–10.
- Giannetti P, Politis M, Su P, Turkheimer FE, Malik O, Keihaninejad S, et al. Increased PK11195-PET binding in normal-appearing white matter in clinically isolated syndrome. *Brain* 2015; 138 (Pt 1): 110–9.
- Gonzalez-Escamilla G, Lange C, Teipel S, Buchert R, Grothe MJ. Alzheimer’s Dis N. PETPVE12: an SPM toolbox for partial volume effects correction in brain PET application to amyloid imaging with AV45-PET. *Neuroimage* 2017; 147: 669–77.
- Goodin DS. Magnetic resonance imaging as a surrogate outcome measure of disability in multiple sclerosis: have we been overly harsh in our assessment? *Ann Neurol* 2006; 59: 597–605.
- Guilarte TR. TSPO in diverse CNS pathologies and psychiatric disease: a critical review and a way forward. *Pharmacol Ther* 2019; 194: 44–58.
- Harrison DM, Roy S, Oh J, Izbudak I, Pham D, Courtney S, et al. Association of cortical lesion burden on 7-T magnetic resonance imaging with cognition and disability in multiple sclerosis. *Jama Neurol* 2015; 72: 1004–12.
- Healy BC, Buckle GJ, Ali EN, Egorova S, Khalid F, Tauhid S, et al. Characterizing clinical and MRI dissociation in patients with multiple sclerosis. *J Neuroimaging* 2017; 27: 481–5.
- Hogel H, Rissanen E, Vuorimaa A, Airas L. Positron emission tomography imaging in evaluation of MS pathology in vivo. *Mult Scler* 2018; 24: 1399–412.
- Jacobsen C, Hagemeyer J, Myhr KM, Nyland H, Lode K, Bergsland N, et al. Brain atrophy and disability progression in multiple sclerosis patients: a 10-year follow-up study. *J Neurol Neurosurg Psychiatry* 2014; 85: 1109–15.
- Kearney H, Rocca MA, Valsasina P, Balk L, Sastre-Garriga J, Reinhardt J, et al. Magnetic resonance imaging correlates of physical disability in relapse onset multiple sclerosis of long disease duration. *Mult Scler* 2014; 20: 72–80. 2019 Nov 4
- Kuhle J, Plavina T, Barro C, Disanto G, Sangurdekar D, Singh CM, et al. Neurofilament light levels are associated with long-term outcomes in multiple sclerosis. *Mult Scler J* 2019. doi: 10.1177/1352458519885613.
- Kutzelnigg A, Lucchinetti CF, Stadelmann C, Brück W, Rauschka H, Bergmann M, et al. Cortical demyelination and diffuse white matter injury in multiple sclerosis. *Brain* 2005; 128 (Pt 11): 2705–12.
- Lukas C, Sombekke MH, Bellenberg B, Hahn HK, Popescu V, Bendfeldt K, et al. Relevance of spinal cord abnormalities to clinical disability in multiple sclerosis: MR imaging findings in a large cohort of patients. *Radiology* 2013; 269: 541–51.
- Minderhoud JM, van der Hoeven JH, Prange AJ. Course and prognosis of chronic progressive multiple sclerosis. Results of an epidemiological study. *Acta Neurol Scand* 1988; 78: 10–5.
- Nutma E, Stephenson JA, Gorter RP, de Bruin J, Boucherie DM, Donat CK, et al. A quantitative neuropathological assessment of translocator protein expression in multiple sclerosis. *Brain* 2019; 142: 3440–55.
- Owen DR, Yeo AJ, Gunn RN, Song K, Wadsworth G, Lewis A, et al. An 18-kDa translocator protein (TSPO) polymorphism explains differences in binding affinity of the PET radioligand PBR28. *J Cereb Blood Flow Metab* 2012; 32: 1–5.
- Politis M, Giannetti P, Su P, Turkheimer F, Keihaninejad S, Wu K, et al. Increased PK11195 PET binding in the cortex of patients with MS correlates with disability. *Neurology* 2012; 79: 523–30.
- Popescu V, Agosta F, Hulst HE, Sluiter IC, Knol DL, Sormani MP, et al. Brain atrophy and lesion load predict long term disability in multiple sclerosis. *J Neurol Neurosurg Psychiatry* 2013; 84: 1082–91.
- Ransohoff RM, Hafler DA, Lucchinetti CF. Corrigendum: multiple sclerosis—a quiet revolution. *Nat Rev Neurol* 2015; 11: 246.
- Rissanen E, Tuisku J, Rokka J, Paavilainen T, Parkkola R, Rinne JO, et al. In vivo detection of diffuse inflammation in secondary progressive multiple sclerosis using PET imaging and the radioligand ¹¹C-PK11195. *J Nucl Med* 2014; 55: 939–44.
- Rissanen E, Tuisku J, Vahlberg T, Sucksdorff M, Paavilainen T, Parkkola R, et al. Microglial activation, white matter tract damage, and disability in MS. *Neurol Neuroimmunol Neuroinflamm* 2018; 5: e443.

- Roussel OG, Ma YL, Evans AC. Correction for partial volume effects in PET: principle and validation. *J Nucl Med* 1998; 39: 904–11.
- Scalfari A, Neuhaus A, Daumer M, Ebers GC, Muraro PA. Age and disability accumulation in multiple sclerosis. *Neurology* 2011; 77: 1246–52.
- Schmidt P, Gaser C, Arsic M, Buck D, Förstner A, Berthele A, et al. An automated tool for detection of FLAIR-hyperintense white-matter lesions in Multiple Sclerosis. *Neuroimage* 2012; 59: 3774–83.
- Scolding N, Barnes D, Cader S, Chataway J, Chaudhuri A, Coles A, et al. Association of British Neurologists: revised (2015) guidelines for prescribing disease-modifying treatments in multiple sclerosis. *Pract Neurol* 2015; 15: 273–9.
- Soelberg Sorensen P, Sellebjerg F. Neurofilament in CSF-A biomarker of disease activity and long-term prognosis in multiple sclerosis. *Mult Scler* 2016; 22: 1112–3.
- Sucksdorff M, Tuisku J, Matilainen M, Vuorimaa A, Smith S, Keitilä J, et al. Natalizumab treatment reduces microglial activation in the white matter of the MS brain. *Neurol Neuroimmunol Neuroinflamm* 2019; 6: e574.
- Thompson AJ, Banwell BL, Barkhof F, Carroll WM, Coetzee T, Comi G, et al. Diagnosis of multiple sclerosis: 2017 revisions of the McDonald criteria. *Lancet Neurol* 2018; 17: 162–73.
- Tremlett H, Zhao Y, Devonshire V. Natural history of secondary-progressive multiple sclerosis. *Mult Scler* 2008; 14: 314–24.
- Tsagkas C, Magon S, Gaetano L, Pezold S, Naegelin Y, Amann M, et al. Spinal cord volume loss: a marker of disease progression in multiple sclerosis. *Neurology* 2018; 91: e349–e58.
- Turkheimer FE, Edison P, Pavese N, Roncaroli F, Anderson AN, Hammers A, et al. Reference and target region modeling of [11C]-(R)-PK11195 brain studies. *J Nucl Med* 2007; 48: 158–67.
- Tutuncu M, Tang J, Zeid NA, Kale N, Crusan DJ, Atkinson EJ, et al. Onset of progressive phase is an age-dependent clinical milestone in multiple sclerosis. *Mult Scler* 2013; 19: 188–98.
- van der Poel M, Ulas T, Mizee MR, Hsiao CC, Miedema SSM, Adelia, et al. Transcriptional profiling of human microglia reveals grey-white matter heterogeneity and multiple sclerosis-associated changes. *Nat Commun* 2019; 10: 1139.
- Varhaug KN, Barro C, Bjørnevik K, Myhr KM, Torkildsen Ø, Wergeland S, et al. Neurofilament light chain predicts disease activity in relapsing-remitting MS. *Neurol Neuroimmunol Neuroinflamm* 2018; 5: e422.
- Vukusic S, Confavreux C. Prognostic factors for progression of disability in the secondary progressive phase of multiple sclerosis. *J Neurol Sci* 2003; 206: 135–7.
- Wattjes MP, Rovira À, Miller D, Yousry TA, Sormani MP, de Stefano MP, et al. Evidence-based guidelines: MAGNIMS consensus guidelines on the use of MRI in multiple sclerosis—establishing disease prognosis and monitoring patients. *Nat Rev Neurol* 2015; 11: 597–606.
- Weinshenker BG, Bass B, Rice GP, Noseworthy J, Carriere W, Baskerville J, et al. The natural history of multiple sclerosis: a geographically based study. 2. Predictive value of the early clinical course. *Brain* 1989; 112 (Pt 6): 1419–28.
- Yaqub M, van Berckel BN, Schuitemaker A, Hinz R, Turkheimer FE, Tomasi G, et al. Optimization of supervised cluster analysis for extracting reference tissue input curves in (R)-[(11)C]PK11195 brain PET studies. *J Cereb Blood Flow Metab* 2012; 32: 1600–8.
- Zivadinov R, Bergsland N, Dwyer MG. Atrophied brain lesion volume, a magnetic resonance imaging biomarker for monitoring neurodegenerative changes in multiple sclerosis. *Quant Imaging Med Surg* 2018; 8: 979–83.
- Zivadinov R, Jakimovski D, Gandhi S, Ahmed R, Dwyer MG, Horakova D, et al. Clinical relevance of brain atrophy assessment in multiple sclerosis. Implications for its use in a clinical routine. *Expert Rev Neurother* 2016; 16: 777–93.